*Int. J. Solids Structures* Vol. 15, pp. 685–699

0020-7683/79/0901-0685/$02.00/0

# DYNAMIC PROPAGATION OF A FINITE CRACK

K. S. KIM
General Electric Company, 3001 East Lake Road, Erie, PA 16531, U.S.A.

(*Received* 8 *May* 1978; *in revised form* 17 *November* 1978)

**Abstract**—A transient analysis of a propagating finite crack of opening mode is considered. A two-dimensional singular integral equation is formulated for the rotation of the crack surface by the method of integral transform. The dynamic stress intensity factor is determined by use of the value of the strength of the square root singularity in the rotation at the crack tip after solving the integral equation numerically. The motion of the crack tips and the load on the crack face are not prescribed in the formulation of the problem. Therefore, the method of solution is applicable to nonuniform rates of propagation of a crack under an arbitrary time dependent load on the crack face. As example problems, the diffraction of a uniform dilatational wave by (1) a stationary crack, (2) a propagating crack with constant speed and (3) a suddenly stopping crack after propagating with constant speed is considered. The dynamic stress intensity is computed for a wide range of time in each problem.

## 1. INTRODUCTION

In plane problems dealing with the dynamic propagation of a crack it is usually assumed that the width of the crack is semi-infinite in order to make the problems tractable. In reality, however, a crack is of finite width. Investigation of the dynamic interaction of the two tips of a finite crack is therefore very important but conventional methods of analysis, for example the Wiener–Hopf technique, are not easily applicable to finite crack problems due to mathematical complexities of the analysis. As a result of lack of adequate tools very little work has been done on dynamic finite crack problems. In this paper, a method will be described to obtain the transient dynamic stress intensity factor for a finite crack whose tips may propagate nonuniformly in time under the action of an arbitrary time dependent normal load on the crack face. It will be shown in the analysis that the rotation of the crack surface can be determined by solving a two-dimensional singular integral equation, and that the dynamic stress intensity factor can be computed by use of the value of the strength of the square root singularity in the rotation at the crack tip. After describing the general method, the diffraction of a uniform dilatational wave by (1) a stationary crack, (2) a propagating crack with constant speed and (3) a suddenly stopping crack after propagating with constant speed will be investigated. Problem (1) has been previously investigated by other authors, thus a comparison of the results is possible. Meanwhile, problems (2) and (3) are still unsolved. The dynamic stress intensity factor vs time curves will be presented for a wide range of time in each problem.

The progress of the work on dynamic crack propagation has been extensively reviewed in recent articles by Achenbach[1] and Freund[2]. The literature in this area can be divided into two categories: steady state problems and transient problems. Steady state problems are, for instance, Yoffee[3], Craggs[4] and Sih and Loeber[5]. Transient problems were, first of all, considered by Baker[6] and Broberg[7]. Baker[6] investigated a semi-infinite crack which suddenly appears in a uniformly stretched elastic medium and then propagates with constant speed. Broberg[7] considered a problem in which a crack initiates at a point and propagates symmetrically with constant speed under constant pressure on the crack face. Attempts to remove the restriction of constant speed of propagation were made by Kostrov[8] and Eshelby[9] for longitudinal shear cracks. Variable speed propagation was also considered by Freund[10] in which a semi-infinite crack extends under a static load normal to the crack plane. Transient analyses of semi-infinite cracks in conjunction with a fracture criterion based on the balance of rate of energy were considered by Achenbach[11] and Achenbach and Nuismer[12]. The effect of wave reflection at the tips of a stationary finite crack was investigated by Thau and Lu[13]. The same problem was also studied by Sih *et al.*[14].

## 2. STATEMENT OF THE PROBLEM

A plane crack is contained in an unbounded medium as shown in Fig. 1. The body is linearly elastic, isotropic and homogeneous. The body force is assumed to be negligible. A Cartesian coordinate system which has been normalized by the actual half crack width is introduced in such a way that the crack surface is initially defined by $-1 < x < 1$, $y = 0\pm$, $-\infty < z < \infty$. The time used in this paper also has been normalized by the time for the dilatational wave to travel half crack width. As a result of these normalizations the dilatational wave speed is equal to 1. The propagation distances of the right and left crack tips are denoted by $a_+(t)$ and $a_-(t)$, respectively. Thus the positions of the crack tips at time $t$ are given by $x = \pm 1 \pm a_\pm(t)$, $y = 0\pm$. The crack tip velocities $\dot{a}_\pm(t)$ are such that $\dot{a}_\pm = 0$ for $t < 0$ and $0 < \dot{a}_\pm(t) < c_R$ for $t > 0$, where $c_R$ is the Rayleigh wave speed. The equations of equilibrium in terms of displacement components are

$$u_{,xx} + \kappa^2 u_{,yy} + (1 - \kappa^2) v_{,xy} = u_{,tt} \tag{1a}$$

$$\kappa^2 v_{,xx} + v_{,yy} + (1 - \kappa^2) u_{,xy} = v_{,tt} \tag{1b}$$

where $\kappa$ is the ratio of the shear wave speed to the dilatational wave speed ($\kappa < 1$), and $u$ and $v$ are the $x$- and $y$-components of displacement, respectively. A subscript comma indicates partial differentiation with respect to the corresponding variables. The stress components normalized by the shear modulus of the material are given by

$$\sigma_{xx} = \frac{1}{\kappa^2} u_{,x} + \left(\frac{1}{\kappa^2} - 2\right) v_{,y}, \tag{2a}$$

$$\sigma_{yy} = \left(\frac{1}{\kappa^2} - 2\right) u_{,x} + \frac{1}{\kappa^2} v_{,y}, \tag{2b}$$

$$\sigma_{xy} = v_{,x} + u_{,y}. \tag{2c}$$

The boundary conditions on the crack surface are

$$\left.\begin{aligned} \sigma_{yy}(x, 0\pm, t) &= \sigma(x, t) \\ \sigma_{xy}(x, 0\pm, t) &= 0 \end{aligned}\right\}, \quad -1 - a_-(t) < x < 1 + a_+(t). \tag{3a, 3b}$$

Due to the symmetry with respect to $y = 0$ we have

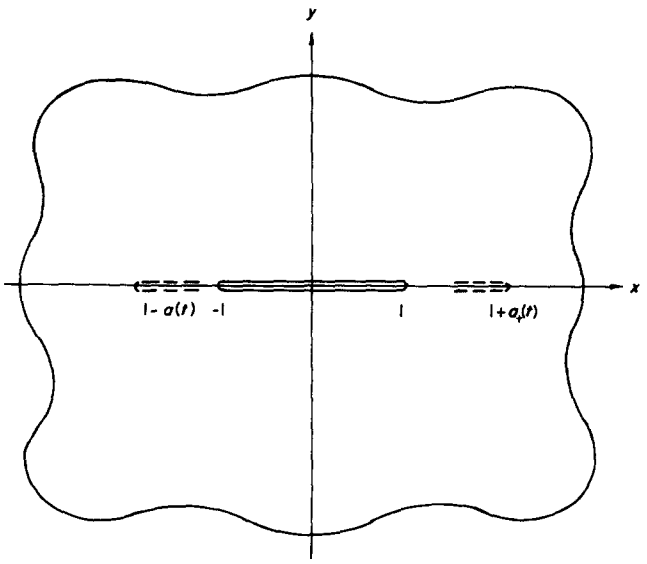


Fig. 1. Model of the problem.

$$\left.\begin{aligned} v(x,0,t)&=0 \\ \sigma_{xy}(x,0,t)&=0 \end{aligned}\right\}, \quad x>1+a_+(t) \quad \text{or} \quad x<-1-a_-(t). \tag{3c, 3d}$$

The initial conditions are

$$u(x,y,0)=0, \tag{4a}$$

$$v(x,y,0)=0, \tag{4b}$$

$$u_{,t}(x,y,0)=0, \tag{4c}$$

$$v_{,t}(x,y,0)=0, \tag{4d}$$

for all $x$ and $y$.

## 3. FORMULATION OF AN INTEGRAL EQUATION

Since the problem is symmetric with respect to $y=0$, we will hereafter consider only the upper half space. We will use $y=0$ instead of $y=0+$ for the $y$-coordinate of the crack face. Integral transforms are employed to reduce the partial differential equations, (1a) and (1b), to ordinary differential equations. First, time $t$ is eliminated by application of the Laplace transform

$$\bar{f}(x,y,p)=\int_0^\infty f(x,y,t)\,\mathrm{e}^{-pt}\,\mathrm{d}t. \tag{5}$$

The initial conditions are used in this transform. Secondly, Fourier trigonometric transforms are used to suppress $y$. They are defined by

$$\hat{\bar{f}}(x,s,p)=\int_0^\infty \bar{f}(x,y,p)\cos(sy)\,\mathrm{d}y, \tag{6a}$$

$$\tilde{\bar{f}}(x,s,p)=\int_0^\infty \bar{f}(x,y,p)\sin(sy)\,\mathrm{d}y. \tag{6b}$$

A Fourier cosine transform is applied to the Laplace transform of eqn (1a), whereas a Fourier sine transform is applied to the Laplace transform of eqn (1b). The resulting equations are

$$\hat{\bar{u}}_{,xx}-\kappa^2\gamma_2{}^2\hat{\bar{u}}+(1-\kappa^2)s\tilde{\bar{v}}_{,x}=(1-2\kappa^2)\bar{v}_{,x}(x,0,p) \tag{7a}$$

$$\tilde{\bar{v}}_{,xx}-\kappa^{-2}\gamma_1{}^2\tilde{\bar{v}}+(1-\kappa^{-2})s\hat{\bar{u}}_{,x}=-s\kappa^{-2}\bar{v}(x,0,p) \tag{7b}$$

where

$$\gamma_1=(s^2+p^2)^{1/2} \tag{8a}$$

$$\gamma_2=(s^2+\kappa^{-2}p^2)^{1/2}. \tag{8b}$$

Boundary conditions (3b) and (3d) together with eqn (2c) have been used to obtain the right-hand sides of eqns (7a) and (7b) in terms of $\bar{v}(x,0,p)$ and $\bar{v}_{,x}(x,0,p)$.

The general solutions of eqns (7a) and (7b) are given by

$$\begin{aligned}\hat{\bar{u}}(x,s,p)&=A_1(s,p)\,\mathrm{e}^{\gamma_1 x}+A_2(s,p)\,\mathrm{e}^{-\gamma_1 x}+A_3(s,p)\,\mathrm{e}^{\gamma_2 x}+A_4(s,p)\,\mathrm{e}^{-\gamma_2 x}\\&\quad+\left[1-\frac{2\gamma_1{}^2}{\gamma_2{}^2-s^2}\right]\int_0^x \bar{v}(\eta,0,p)\cosh[\gamma_1(\eta-x)]\,\mathrm{d}\eta\\&\quad+\frac{2s^2}{\gamma_2{}^2-s^2}\int_0^x \bar{v}(\eta,0,p)\cosh[\gamma_2(\eta-x)]\,\mathrm{d}\eta,\end{aligned} \tag{9a}$$

$$\tilde{\bar{v}}(x,s,p)=-\frac{s}{\gamma_1}A_1(s,p)\,\mathrm{e}^{\gamma_1 x}+\frac{s}{\gamma_1}A_2(s,p)\,\mathrm{e}^{-\gamma_1 x}-\frac{\gamma_2}{s}A_3(s,p)\,\mathrm{e}^{\gamma_2 x}+\frac{\gamma_2}{s}A_4(s,p)\,\mathrm{e}^{-\gamma_2 x}$$

$$+\frac{s}{\gamma_1}\left[1-\frac{2\gamma_1^2}{\gamma_2^2-s^2}\right]\int_0^x \bar{v}(\eta,0,p)\sinh[\gamma_1(\eta-x)]\,d\eta$$

$$+\frac{2s\gamma_2}{\gamma_2^2-s^2}\int_0^x \bar{v}(\eta,0,p)\sinh[\gamma_2(\eta-x)]\,d\eta. \tag{9b}$$

The coefficients $A_1$, $A_2$, $A_3$ and $A_4$ are determined from the conditions

$$\hat{\bar{u}}(x,s,p)=0, \qquad \text{at } x=\pm\infty, \tag{10a}$$

$$\hat{\bar{v}}(x,s,p)=0, \qquad \text{at } x=\pm\infty. \tag{10b}$$

We get

$$A_1(s,p)=-\tfrac{1}{2}\left[1-\frac{2\gamma_1^2}{\gamma_2^2-s^2}\right]\int_0^\infty \bar{v}(\eta,0,p)\,e^{-\gamma_1\eta}\,d\eta, \tag{11a}$$

$$A_2(s,p)=\tfrac{1}{2}\left[1-\frac{2\gamma_1^2}{\gamma_2^2-s^2}\right]\int_{-\infty}^0 \bar{v}(\eta,0,p)\,e^{\gamma_1\eta}\,d\eta, \tag{11b}$$

$$A_3(s,p)=-\frac{s^2}{\gamma_2^2-s^2}\int_0^\infty \bar{v}(\eta,0,p)\,e^{-\gamma_2\eta}\,d\eta, \tag{11c}$$

$$A_4(s,p)=\frac{s^2}{\gamma_2^2-s^2}\int_{-\infty}^0 \bar{v}(\eta,0,p)\,e^{\gamma_2\eta}\,d\eta. \tag{11d}$$

Stress components in the transform space, $\hat{\bar{\sigma}}_{xx}$, $\hat{\bar{\sigma}}_{yy}$ and $\hat{\bar{\sigma}}_{xy}$, can be obtained by transforming eqns (2a), (2b) and (2c) accordingly and substituting $\hat{\bar{u}}$ and $\hat{\bar{v}}$. In this study, however, we will only consider $\hat{\bar{\sigma}}_{yy}$, since our main interest is in the determination of the dynamic stress intensity factor. $\hat{\bar{\sigma}}_{yy}$ is given by

$$\hat{\bar{\sigma}}_{yy}=\left(\frac{1}{\kappa^2}-2\right)\hat{\bar{u}}_{,x}+\frac{s}{\kappa^2}\hat{\bar{v}}-\frac{1}{\kappa^2}\bar{v}(x,0,p). \tag{12}$$

Substituting $\hat{\bar{u}}$ and $\hat{\bar{v}}$ into eqn (12) and integrating by parts, we obtain

$$\begin{aligned}\hat{\bar{\sigma}}_{yy}(x,s,p)=&\tfrac{1}{2}\left[\left(2-\frac{1}{\kappa^2}\right)+\frac{s^2}{\kappa^2\gamma_1^2}\right]\left[1-\frac{2\gamma_1^2}{\gamma_2^2-s^2}\right]\int_x^\infty \bar{v}_{,\eta}(\eta,0,p)\,e^{-\gamma_1(\eta-x)}\,d\eta\\
&-\tfrac{1}{2}\left[\left(2-\frac{1}{\kappa^2}\right)+\frac{s^2}{\kappa^2\gamma_1^2}\right]\left[1-\frac{2\gamma_1^2}{\gamma_2^2-s^2}\right]\int_{-\infty}^x \bar{v}_{,\eta}(\eta,0,p)\,e^{\gamma_1(\eta-x)}\,d\eta\\
&+\frac{2s^2}{\gamma_2^2-s^2}\int_x^\infty \bar{v}_{,\eta}(\eta,0,p)\,e^{-\gamma_2(\eta-x)}\,d\eta\\
&-\frac{2s^2}{\gamma_2^2-s^2}\int_{-\infty}^x \bar{v}_{,\eta}(\eta,0,p)\,e^{\gamma_2(\eta-x)}\,d\eta\\
&-\frac{p^2}{\kappa^2\gamma_1^2}\bar{v}(x,0,p).\end{aligned} \tag{13}$$

The inverse Fourier cosine transform which is defined by

$$\bar{f}(x,y,p)=\frac{2}{\pi}\int_0^\infty \hat{\bar{f}}(x,s,p)\cos(sy)\,ds \tag{14}$$

is performed on eqn (13) for $y=0$. Then we take the inverse Laplace transform by application of the Cagniard–De Hoop method, that is, the expression for $\bar{\sigma}_{yy}$ obtained above is changed into

a recognizable Laplace transform by setting $\gamma_i|\eta - x| = pt$, $i = 1, 2$, in each double integral. Then, using the identity

$$\overline{\left[\frac{\partial}{\partial t} f*g(t)\right]} = p\bar{f}\bar{g}, \tag{15}$$

where $*$ implies the convolution integral, we obtain

$$\begin{aligned}\sigma_{yy}(x,0,t) = \frac{\partial}{\partial t}\Bigg[&\int_{-\infty}^{\infty}\int_0^t v_{,\eta}(\eta,0,\tau)H(t-\tau-|\eta-x|)M_1(t-\tau,\eta-x)\,d\tau\,d\eta\\ &+\int_{-\infty}^{\infty}\int_0^t v_{,\eta}(\eta,0,\tau)H\left(t-\tau-\frac{|\eta-x|}{\kappa}\right)M_2(t-\tau,\eta-x)\,d\tau\,d\eta\\ &-\frac{1}{\kappa^2}\int_{-\infty}^{x} v_{,\eta}(\eta,0,t)\,d\eta\Bigg],\end{aligned} \tag{16}$$

where

$$\begin{aligned}M_1(\xi,\zeta) &= \frac{4}{\pi}\left[\frac{\xi}{\zeta}-\frac{1}{4\kappa^2}\left(\frac{\xi}{\zeta}\right)^2-\kappa^2\left(\frac{\xi}{\zeta}\right)^3\right][\xi^2-\zeta^2]^{-1/2},\\ M_2(\xi,\zeta) &= \frac{4}{\pi}\kappa^2\frac{\xi}{\zeta^3}\left[\xi^2-\frac{\zeta^2}{\kappa^2}\right]^{1/2},\end{aligned} \tag{17}$$

and $H(t)$ is the Heaviside function. Equation (16) is rearranged in such a way that the terms with the Cauchy kernel $(\eta - x)^{-1}$ are extracted out and the terms with the kernel $(\eta - x)^{-3}$ in $M_1$ and $M_2$ are combined together so that the strong singularities across $\eta = x$ are cancelled. Noticing that $v_{,\eta}(\eta, 0, \tau)$ is equal to the rotation of the crack surface, $\omega(\eta, 0, \tau)$, because of eqns (3b), we obtain the following equation:

$$\sigma_{yy}(x,0,t) = \frac{4}{\pi}\frac{\partial}{\partial t}J(x,t), \tag{18}$$

where

$$\begin{aligned}J(x,t) = -\kappa^2 &\iint_{A_1-A_2}\omega(\eta,0,\tau)\frac{(t-\tau)^2}{(\eta-x)^3}\,d\tau\,d\eta\\ &+(1-\tfrac{1}{2}\kappa^2)\int\int_{A_1}\omega(\eta,0,\tau)\frac{1}{(\eta-x)}\,d\tau\,d\eta\\ &-\tfrac{1}{2}\int\int_{A_2}\omega(\eta,0,\tau)\frac{1}{(\eta-x)}\,d\tau\,d\eta\\ &+\int\int_{A_1}\omega(\eta,0,\tau)\frac{K_1(t-\tau,\eta-x)}{[(t-\tau)^2-(\eta-x)^2]^{1/2}}\,d\tau\,d\eta\\ &+\int\int_{A_2}\omega(\eta,0,\tau)K_2(t-\tau,\eta-x)\,d\tau\,d\eta\\ &-\frac{\pi}{4\kappa^2}\int_{-1-a_-(t)}^{x}\omega(\eta,0,t)\,d\eta,\end{aligned} \tag{19}$$

where

$$K_1(\xi,\zeta) = \left(\frac{\zeta}{\xi}\right)\left\{\frac{1}{1+\left[1-\left(\frac{\zeta}{\xi}\right)^2\right]^{1/2}}-\frac{1}{4\kappa^2}-\frac{\kappa^2}{4}\frac{\left(\frac{\zeta}{\xi}\right)^2+3}{1+\left[1+\frac{1}{2}\left(\frac{\zeta}{\xi}\right)^2\right]\left[1-\left(\frac{\zeta}{\xi}\right)^2\right]^{1/2}}\right\},$$

$$K_2(\xi,\zeta) = -\frac{1}{2\kappa^2}\left(\frac{\zeta}{\xi}\right)\left\{1+\left[1-\frac{1}{\kappa^2}\left(\frac{\zeta}{\xi}\right)^2\right]^{1/2}\right\}^{-2}\frac{1}{\xi}, \tag{20}$$

and $A_1$ and $A_2$ are the domains of dependence defined by

$$A_1 = \{(\eta, \tau) | \quad 0 < \tau < t - |\eta - x|, \quad -1 - a_-(\tau) < \eta < 1 + a_+(\tau)\},$$

$$A_2 = \left\{(\eta, \tau) | \quad 0 < \tau < t - \frac{|\eta - x|}{\kappa}, \quad -1 - a_-(\tau) < \eta < 1 + a_+(\tau)\right\}.$$

The $\eta$-integration in the second and third terms in eqn (19) which include the Cauchy kernels is performed in the sense of the Cauchy principal value, if they do not exist in the sense of Riemann. Recalling that $\sigma_{yy}(x, 0, t)$ is given as a boundary condition on the crack face, eqn (18) can be viewed as a differential-integral equation for the unknown function $\omega(\eta, 0, \tau)$. Evaluation of $\omega(\eta, 0, \tau)$ can only be carried out numerically since the equation is not tractable. To facilitate the application of our numerical technique we now change eqn (18) into the form of an integral equation by integrating with respect to time. Noticing that

$$\int_0^{t_c} \sigma_{yy}(x, 0, \tau)\, d\tau = \frac{4}{\pi} J(x, t_c) \tag{21}$$

for $|x| > 1$, where $t_c$ is the time when the propagating crack tip arrives at $x$, that is, $x = 1 + a_+(t_c)$ if $x > 1$, $x = -1 - a_-(t_c)$ if $x < -1$, we obtain

$$\frac{4}{\pi}[J(x, t) - H(|x| - 1)J(x, t_c)] = \int_{t_c}^{t} \sigma_{yy}(x, 0, \tau)\, d\tau. \tag{22}$$

In eqn (22) we assume that $t_c = 0$ if $|x| < 1$.

To evaluate $\omega(\eta, 0, \tau)$ in eqn (22), it will be expedient to have some information on the behavior of $\omega$ *a priori* and set the function into the form in which the singularities of $\omega$ appear explicitly. Two types of singularities are expected in view of some previous analyses in the literature. The first type is the square root singularity which arises at the crack tip. The proof of this fact can be found in Achenbach and Bazant[15] and Freund and Clifton[16]. The second type of singularity is the travelling logarithmic singularity which is located at the front of the Rayleigh wave. We can find this singularity in Baker[6] and Thau and Lu[14] by differentiating normal displacement of the crack face with respect to the coordinate of crack propagation direction. Representation of this type of singularity, however, makes the expression too cumbersome. Also, for a finite crack no information is available to date on the behavior of the travelling singularities after rediffraction of the cylindrical waves at the crack tips. For these reasons we neglect the travelling singularities in the structure of $\omega$, and write $\omega$ simply as

$$\omega(\eta, 0, \tau) = \frac{\Omega(\eta, \tau)}{[1 + a_+(\tau) - \eta]^{1/2}[1 + a_-(\tau) + \eta]^{1/2}}, \tag{23}$$

where $\Omega$ is assumed to be bounded and continuous almost everywhere over the area $A$ defined by $A = \{(\eta, \tau) | \tau \geqq 0, -1 - a_-(\tau) < \eta < 1 + a_+(\tau)\}$. $\Omega$ is zero if $(\eta, \tau)$ is not in $A$. Therefore, there is a jump discontinuity in $\Omega$ across the crack tip trajectories. In order to derive a formula for the stress intensity factor, we will further assume that $\Omega$ is analytic in $A$ almost everywhere along the crack tip trajectories. Furthermore, in the numerical computation process of the integral equation we will treat $\Omega$ as if it is bounded and continuous everywhere in $A$. Deviation of the numerical results from some existing data by this treatment is thought to be insignificant as will be shown in example problems.

## 4. STRESS INTENSITY FACTOR

The dynamic stress intensity factor, $K_{ID}(t)$, is defined by

$$K_{ID}^{\pm}(t) = \lim_{\epsilon \to 0+} \sqrt{(2\pi\epsilon)}\sigma_{yy}[\pm 1 \pm a_{\pm}(t) \pm \epsilon, t], \tag{24}$$

where the upper and lower signs are for the right and left crack tips, respectively. We now consider the evaluation of $K_{ID}^{\pm}$ for uniform extension of a crack. The formula obtained for this case will be extended to nonuniform propagation of the crack without detailed proof. For uniform extension, eqn (23) is written as

$$\omega(\eta, 0, \tau) = \frac{\Omega(\eta, \tau)}{[(1+c\tau)^2 - \eta^2]^{1/2}}. \tag{25}$$

Let us first consider $K_{ID}^{+}$. Substituting eqn (18) into eqn (24), $K_{ID}^{+}$ becomes

$$K_{ID}^{+}(t) = \frac{4}{\pi} \lim_{x \to (1+ct)+} \sqrt{(2\pi(x-1-ct))} \frac{\partial}{\partial t} J(x, t). \tag{26}$$

In order to evaluate the right hand side of eqn (26), let us take a particular point $(x, t)$ in the $\eta - \tau$ plane such that $x > 1 + ct$ [see Figs. 2(a) and 2(b)] and construct $A_1$ and $A_2$. Then introduce $(N, T)$ and $(r, \theta)$ coordinate systems as illustrated. Then divide $A_1$ into $A_{11}$ and $A_{12}$, where $A_{11}$ is the area generated by drawing a circle with its center at $(x, t)$ and radius $r_1$. $A_{11}$ includes the point $(\eta_1, \tau_1)$ which is the intersection of $t - \tau = x - \eta$ and $\eta = 1 + c\tau$. Similarly, we divide $A_2$ into $A_{21}$ and $A_{22}$ as shown in Fig. 2(b). Let us denote the contribution of $i$th term in $J(x, t)$ to $K_{ID}^{+}$ by $J_i$. For $i = 1$, using eqn (25), we have

$$J_1 = -\frac{4}{\pi} \kappa^2 \lim_{x \to (1+ct)+} \sqrt{(2\pi(x-1-ct))} \frac{\partial}{\partial t} \left[ \int\int_{A_{11}} + \int\int_{A_{12}} - \int\int_{A_{21}} - \int\int_{A_{22}} \right]$$

$$\frac{\Omega(\eta, \tau)}{\sqrt{((1+c\tau)^2 - \eta^2)}} \frac{(t-\tau)^2}{(\eta - x)^3} \, d\tau \, d\eta. \tag{27}$$

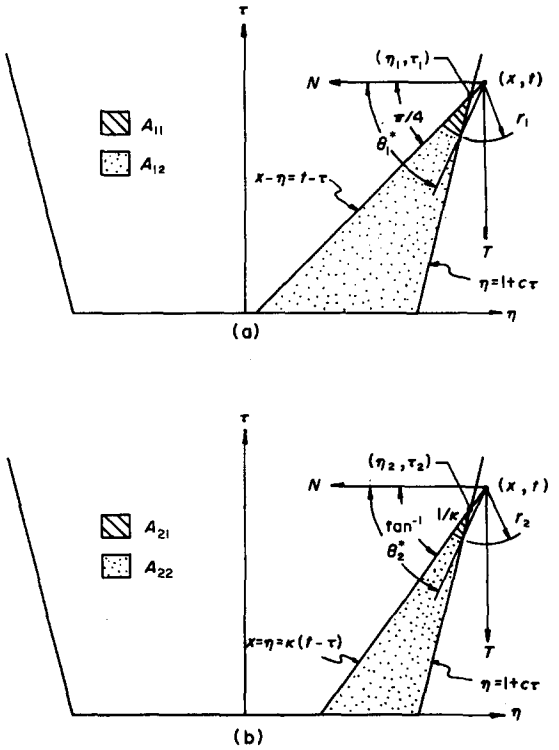


Fig. 2. Division of the area of integration for evaluation of $K_{ID}^{+}$.

Denoting the contribution of each integral in the bracket of this equation to $J_1$ by $J_{1i}$, where $i = 1, 2, 3, 4$, then we find $J_{12} = J_{14} = 0$ by direct differentiation of the integrals and passage to the limit. Using the polar coordinate system and expanding $\Omega$ into a Taylor series about $(\eta_1, \tau_1)$, $J_{11}$ can be written as

$$J_{11} = \frac{4}{\pi}\kappa^2 \lim_{x\to(1+ct)+} \sqrt{(2\pi(x-1-ct))}\frac{\partial}{\partial t}\left[\frac{\Omega(\eta_1,\tau_1)}{\sqrt{(1+c\tau_1+\eta_1)}}\int_{\pi/4}^{\theta_1^\dagger}\frac{\sin^2\theta\,d\theta}{\cos^3\theta}\right.$$
$$\left.\int_{r_0}^{r_1}\frac{dr}{\sqrt{(1+c(t-r\sin\theta)-(x-r\cos\theta))}}+\Phi(x,t)\right] \tag{28}$$

where $r_0(x-1-ct)/(\cos\theta - c\sin\theta)$ is the distance from $(x, t)$ to $\eta = 1 + c\tau$ along any fixed $\theta$, $\theta_1^\dagger$ is the angle at the intersection of $r = r_1$ and $\eta = 1 + c\tau$, and $\Phi(x, t)$ is such that $\sqrt{(x-1-ct)}\Phi_{,t} \to 0$ as $x \to (1+ct)+$. After performing $r$-integration and introducing a new variable $\xi$ defined by $\xi = x - r_1(\cos\theta - c\sin\theta)$, we obtain

$$J_{11} = -\frac{4}{\pi}\kappa^2 c \lim_{x\to(1+ct)+}\sqrt{(2\pi(x-1-ct))}\frac{\Omega(1+ct,t)}{\sqrt{(2(1+ct))}}\int_{\xi_0}^{\xi_1^\dagger}\frac{\tan^2\theta(1+\tan^2\theta)\,d\xi}{(\tan\theta+c)(\xi-x)\sqrt{(\xi_1^\dagger-\xi)}}. \tag{29}$$

where $\xi_1^\dagger = x - r_1(\cos\theta_1^\dagger - c\sin\theta_1^\dagger) = 1 + ct$ and $\xi_0 = x - r_1(\cos\pi/4 - c\sin\pi/4)$. Then, referring to Mushkelishvili[17] and observing that $\lim_{x\to(1+ct)+}\tan\theta_1^\dagger = 1/c$, we finally obtain

$$J_{11} = \frac{4\sqrt{(\pi)}\kappa^2}{c^2}\frac{\Omega(1+ct,t)}{\sqrt{(1+ct)}}. \tag{30}$$

Similarly, we can show $J_{13} = -J_{11}$, and so $J_1 = 0$. The evaluation of $J_2$, $J_3$, $J_4$ and $J_5$ are accomplished in an analogous manner. Consequently, only the results are presented here:

$$J_2 = -4\sqrt{(\pi)}(1-\tfrac{1}{2}\kappa^2)\frac{\Omega(1+ct,t)}{\sqrt{(1+ct)}}, \tag{31}$$

$$J_3 = 2\sqrt{(\pi)}\frac{\Omega(1+ct,t)}{\sqrt{(1+ct)}}, \tag{32}$$

$$J_4 = -4\sqrt{(\pi)}\frac{c^2}{\sqrt{(1-c^2)}}\left\{\frac{1}{1+\sqrt{(1-c^2)}}-\frac{1}{4\kappa^2}-\frac{\kappa^2(3+c^2)}{4[1+(1+c^2/2)\sqrt{(1-c^2)}]}\right\}\frac{\Omega(1+ct,t)}{\sqrt{(1+ct)}}, \tag{33}$$

$$J_5 = 2\sqrt{(\pi)}\left(\frac{c}{\kappa}\right)^2\left[1+\sqrt{\left(1-\left(\frac{c^2}{\kappa}\right)\right)}\right]^{-2}\frac{\Omega(1+ct,t)}{\sqrt{(1+ct)}}. \tag{34}$$

The last term, $J_6$, vanishes since $v(-1-ct, t) = 0$ and $v(x, t) = 0$. Adding all of the $J_i$'s, the dynamic stress intensity factor becomes

$$K_{ID}^+(t) = f(\kappa, c)\frac{\Omega(1+ct,t)}{\sqrt{(1+ct)}}, \tag{35}$$

where

$$f(\kappa,c) = -2\sqrt{(\pi)}(1-\kappa^2) - \frac{4\sqrt{(\pi)}c^2}{\sqrt{(1-c^2)}}\left\{\frac{1}{1+\sqrt{(1-c^2)}}-\frac{1}{4\kappa^2}-\frac{\kappa^2(3+c^2)}{4[1+(1+c^2/2)\sqrt{(1-c^2)}]}\right\}$$
$$+2\sqrt{(\pi)}\left(\frac{c}{\kappa}\right)^2\left[1+\sqrt{\left(1-\left(\frac{c}{\kappa}\right)^2\right)}\right]^{-2}. \tag{36}$$

In a similar manner, we obtain

$$K_{ID}^-(t) = -f(\kappa,c)\frac{\Omega(-1-ct,t)}{\sqrt{(1+ct)}} \tag{37}$$

for the left crack tip.

Recalling that $K_{ID}^{+}$ was determined by considering a neighborhood of the point $(1+ct, t)$ in the $\eta$–$\tau$ plane, we can extend the applicability of eqns (35) and (37) to nonuniform rates of propagation with some modification. We obtain the following equation:

$$K_{ID}^{\pm}(t) = \pm f[\kappa, \dot{a}_{\pm}(t)] \frac{\Omega[\pm 1 \pm a_{\pm}(t), t]}{\sqrt{([2 + a_{-}(t) + a_{+}(t)]/2)}}. \tag{38}$$

To determine $K_{ID}(t)$ we first obtain $[\pm 1 \pm a_{\pm}(t), t]$ by solving the integral eqn (22) numerically. Then, we compute $K_{ID}^{\pm}(t)$ by utilizing the above equation.

## 5. EXAMPLE PROBLEMS

As numerical examples, we will investigate the diffraction of a uniform dilatational wave with propagation vector normal to the crack plane by (1) a stationary crack, (2) a crack propagating symmetrically with constant speed, and (3) a suddenly stopping crack after propagating symmetrically with constant speed. The total wave field for a diffraction problem is determined by adding the incident wave field and the scattered wave field. For the purpose of determining the stress intensity factor we only need to consider the scattered wave field. The boundary condition (3a) for the scattered wave field is given by

$$\sigma_{yy}(x, 0, t) = -\sigma_0 H(t - t_c), \qquad \text{for } |x| < 1 + a(t), \tag{39}$$

where $\sigma_0$ is the uniform pressure on the crack face, and $a(t) = a_{-}(t) = a_{+}(t)$. $a(t)$ is defined by

$$a(t) = \begin{cases} 0, & \text{problem (1)}, \\ ct, & \text{problem (2)}, \\ ct, & t < t_A \\ ct_A, & t \geqq t_A \end{cases} \quad \text{problem (3)}, \tag{40}$$

where $t_A$ is the time when the crack stops suddenly. The numerical scheme for computation of the integral eqn (22) is outlined in the following: Introduce a new variable $\eta^*$ defined by $\eta^* = \eta/[1 + a(\tau)]$, and map $A_1$ and $A_2$ onto $A_1^*$ and $A_2^*$, respectively (see Fig. 3). Then, divide $A_1^*$ and $A_2^*$ into a set of horizontal strips. Neglecting the logarithmic singularities as mentioned earlier, we approximate $\Omega^*$ in each strip by

$$\Omega^*(\eta^*, \tau) \approx \sum_{j=1,3,\ldots}^{2N-1} [a_{kj} + b_{kj}(\tau - \tau_k)] T_j(\eta^*), \quad \tau_k \leqq \tau \leqq \tau_{k+1}, \tag{41}$$

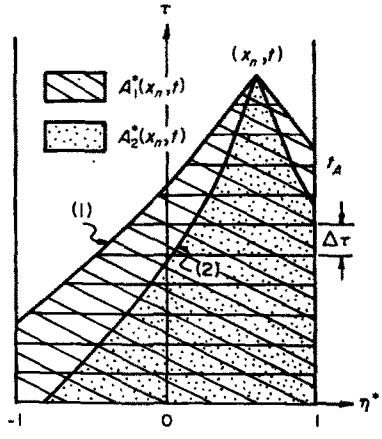


Fig. 3. Division of the area of integration for numerical integration.

(1) $|(1 + c\tau)\eta^* - x_n| = t - \tau, \quad \tau \leqq t_A$
$|(1 + ct_A)\eta^* - x_n| = t - \tau, \quad \tau > t_A$

(2) $|(1 + c\tau)\eta^* - x_n| = \kappa(t - \tau), \quad \tau \leqq t_A$
$|(1 + ct_A)\eta^* - x_n| = \kappa(t - \tau), \quad \tau > t_A.$

where $\Omega^*(\eta^*, \tau) = \Omega(\eta, \tau)$, $a_{kj}$ and $b_{kj}$ are constants and $T_j$ is the $j$th order Chebyshev polynomial of the first kind. Note that only odd order polynomials are included in eqn (41). This is due to the anti-symmetry of the rotation with respect to $y$-axis for the problems under consideration. Taking $\tau_1 = 0$, then $a_{1j} = 0$ from the initial conditions. Also, from the continuity of $\Omega^*$ at $\tau = \tau_k$, we have $a_{kj} = a_{lj} + b_{lj}(\tau k - \tau_l)$, where $l = k - 1$. The problem is now reduced to determine $b_{kj}$'s in each strip. In order to compute $b_{ij}(\tau_1 < \tau < \tau_{i+1} = t)$, pick $N$ values of $x$ which are zeros of $T_{2N-1}\{x/[1 + a(t)]\}$ in $[0, 1 + a(t)]$, namely

$$x_n = [1 + a(t)] \cos\left(\frac{2n - 1}{2N - 1}\frac{\pi}{2}\right). \tag{42}$$

where $n = 1, 2, \ldots, N$. Then, substituting eqn (41) into eqn (22), we obtain the following $N \times N$ linear system of equations:

$$\sum_{k=1}^{i} \sum_{j=1,3,\ldots}^{2N-1} [a_{kj}F_{j1k}(x_n, t) + b_{kj}F_{j2k}(x_n, t)] - \frac{\pi}{4}\frac{1}{\kappa^2} \sum_{j=1,3,\ldots}^{2N-1} [a_{ij} + b_{ij}(t - \tau_i)]$$

$$\times \int_{-1}^{x_n/1+a(t)} \frac{T_j(\eta^*)}{\sqrt{(1 - \eta^{*2})}}\, d\eta^* - H(|x_n| - 1) \sum_{k=1}^{k_c} \sum_{j=1,3,\ldots}^{2N-1} [a_{jk}F_{j1k}(x_n, t_c) + b_{kj}F_{j2k}(x_n, t_c)] = -(t - t_c) \tag{43}$$

where $n = 1, 2, \ldots, N$,

$$\begin{aligned} F_{jlk}(x_n, t) = -\kappa^2 & \iint_{A_{1k}^{\dagger} - A_{2k}^{\dagger}} \frac{T_j(\eta^*)}{\sqrt{(1 - \eta^{*2})}} \frac{f_{lk}(\tau)(t - \tau)^2}{[(1 + c\tau)\eta^* - x_n]^3}\, d\tau\, d\eta^* \\ & + (1 - \tfrac{1}{2}\kappa^2) \iint_{A_{1k}^{\dagger}} \frac{T_j(\eta^*)}{\sqrt{(1 - \eta^{*2})}} \frac{f_{lk}(\tau)}{[(1 + c\tau)\eta^* - x_n]}\, d\tau\, d\eta^* \\ & - \frac{1}{2}\int_{A_{2k}^{\dagger}} \int \frac{T_j(\eta^*)}{\sqrt{(1 - \eta^{*2})}} \frac{f_{lk}(\tau)}{[(1 + c\tau)\eta^* - x_n]}\, d\tau\, d\eta^* \\ & + \int_{A_{1k}^{\dagger}} \int \frac{T_j(\eta^*)}{\sqrt{(1 - \eta^{*2})}} \frac{f_{lk}(\tau) K_1[t - \tau, (1 + c\tau)\eta^* - x_n]}{\sqrt{((t - \tau)^2 - [(1 + c\tau)\eta^* - x_n]^2)}}\, d\tau\, d\eta^* \\ & + \int_{A_{2k}^{\dagger}} \int \frac{T_j(\eta^*)}{\sqrt{(1 - \eta^{*2})}} f_{lk}(\tau) K_2[t - \tau, (1 + c\tau)\eta^* - x_n]\, d\tau\, d\eta^*. \end{aligned} \tag{44}$$

where $f_{1k}(\tau) = 1$, $f_{2k}(\tau) = \tau - \tau_k$, $A_{1k}^{\dagger}$ and $A_{2k}^{\dagger}$ are the areas of the $k$th strip associated with $A_1^{\dagger}$ and $A_2^{\dagger}$, respectively, and $k_c$ is the number of the strip in which $\tau_{k_c} < t_c \leqq \tau_{k_c+1}$.

The area integrals $F_{jlk}$ are computed approximately by application of the quadrature formulas of Gauss type except the $\eta^*$-integrals in the second and third terms which are computed analytically by use of the recurrence formula $T_{j+1}(x) = 2xT_j(x) + T_{j-1}(x)$. The detail of the integration procedure is described in [18]. Typical examples of the numerical results for $\Omega^*$ are presented in Figs. 4 and 5 for $\sigma_0 = 4/\pi$. The results were satisfactory for stationary and suddenly stopping cracks, however severe oscillation, as seen in the figures, was produced for the propagating crack as crack speed increased. The oscillation was somewhat dependent upon the order of polynomial and the size of time increment but no drastic improvement was found. It is felt that a more refined numerical scheme would be necessary to remove the oscillation. In the interpretation of the data it was assumed that the true behavior of $\Omega^*$ is represented by the central curves which passes through the middle of oscillation. These curves are indicated by dotted lines in the figures. Before proceeding with the discussion of the results for $K_{ID}$, let us define the normalized dynamic stress intensity factor, $K_{ID}^{\dagger}(t)$, by dividing $K_{ID}(t)$ by the quasi-static stress intensity factor, $\sigma_0\sqrt{(\pi[1 + a(t)])}$. For $\sigma_0 = 4/\pi$, $K_{ID}^{\dagger}$ in terms of $\Omega^*$ becomes

$$K_{ID}^{\dagger}(t) = \frac{\pi}{4} f(\kappa, \dot{a})\Omega^*(1, t)/[1 + a(t)]. \tag{45}$$

The $K_{ID}^{\dagger}$ vs time curves are presented in Figs. 6–9.

The notation for specific times which appear in the figures is defined in the following:

$t_P(t_S, t_R)$ = the time for the first scattered dilatational (shear, Rayleigh) wave to traverse the crack width.

$t_{PP} = t_P$ + the time for the first rescattered dilatational wave ($PP$ wave) to traverse the crack width.

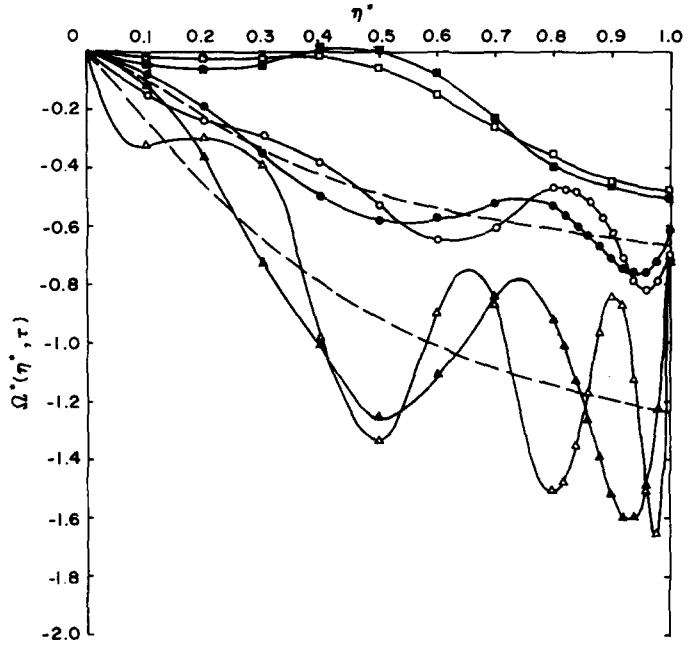


Fig. 4. The profile of $\Omega^*(\eta^*, \tau)$ (small times). $\kappa = 0.542$. □; $2N-1=5$, $\Delta\tau = 0.2$, $\Delta\eta^* = 0.2$, $c = 0$, $\tau = 1.0$. ■; $2N-1=9$, $\Delta\tau = 0.2$, $\Delta\eta^* = 0.2$, $c = 0$, $\tau = 1.0$. ○; $2N-1=11$, $\Delta\tau = 0.2$, $\Delta\eta^* = 0.2$, $c = 0.4\kappa$, $\tau = 2.0$. ●; $2N-1=9$, $\Delta\tau = 0.4$, $\Delta\eta^* = 0.2$, $c = 0.4\kappa$, $\tau = 2.0$. △; $2N-1=15$, $\Delta\tau = 0.2$, $\Delta\eta^* = 0.2$, $c = 0.8\kappa$, $\tau = 4.0$. ▲; $2N-1=9$, $\Delta\tau = 0.4$, $\Delta\eta^* = 0.2$, $c = 0.8\kappa$, $\tau = 4.0$. ——; Approximate curves.

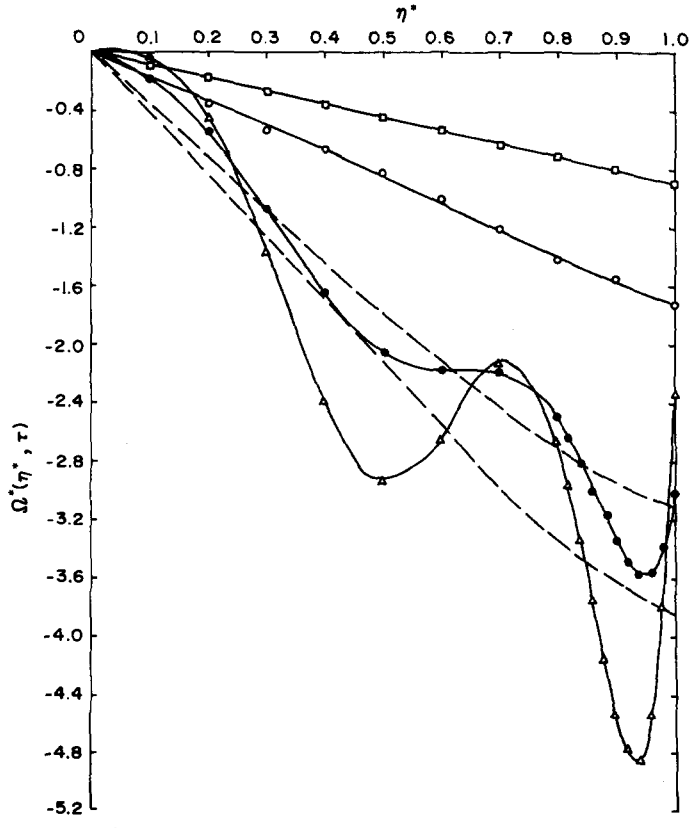


Fig. 5. The profile of $\Omega^*(\eta^*, \tau)$ (large times). $\kappa = 0.542$. □; $2N-1=5$, $\Delta\tau = 0.2$, 0.5, $\Delta\eta^* = 0.2$, $c = 0$, $\tau = 14.7$. ○; $2N-1=9$, $\Delta\tau = 0.4$, $\Delta\eta^* = 0.2$, $t_A = 1.2$, $c = 0.8\kappa$, $\tau = 10.0$. ●; $2N-1=9$, $\Delta\tau = 0.4$, $\Delta\eta^* = 0.2$, $c = 0.4\kappa$, $\tau = 14.8$. △; $2N-1=9$, $\Delta\tau = 0.4$, $\Delta\eta^* = 0.2$, $c = 0.8\kappa$, $\tau = 14.8$. ——; Approximate curves.

$t_{RA} = t_A +$ the time for the Rayleigh wave generated at $t = t_A$ to traverse the crack width.

For the time interval $0 < t < t_P$ where no wave interaction occurs the results for the stationary and propagating cracks must agree with the results for a semi-infinite crack in Baker[6]. $K^*_{ID}$ obtained from Baker's equation for $\sigma_{yy}$ can be expressed as

$$K^*_{ID}(t) = k(\kappa, c)\sqrt{\left(\frac{t}{1+ct}\right)}. \tag{46}$$

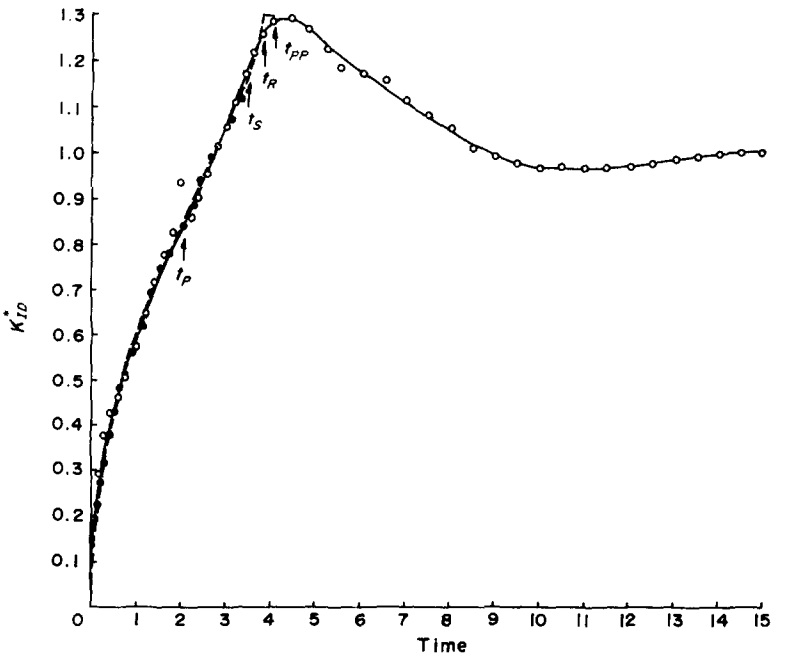


Fig. 6. The normalized dynamic stress intensity factor of a stationary crack $\kappa = 0.577$ ($\nu = 0.25$). ——; Thau and Lu[13]. ——; This study. ○; $2N - 1 = 5$, $\Delta\tau = 0.2, 0.5$, $\Delta\eta^* = 0.2$. ●; $2N - 1 = 9$, $\Delta\tau = 0.1$, $\Delta\eta^* = 0.2$.

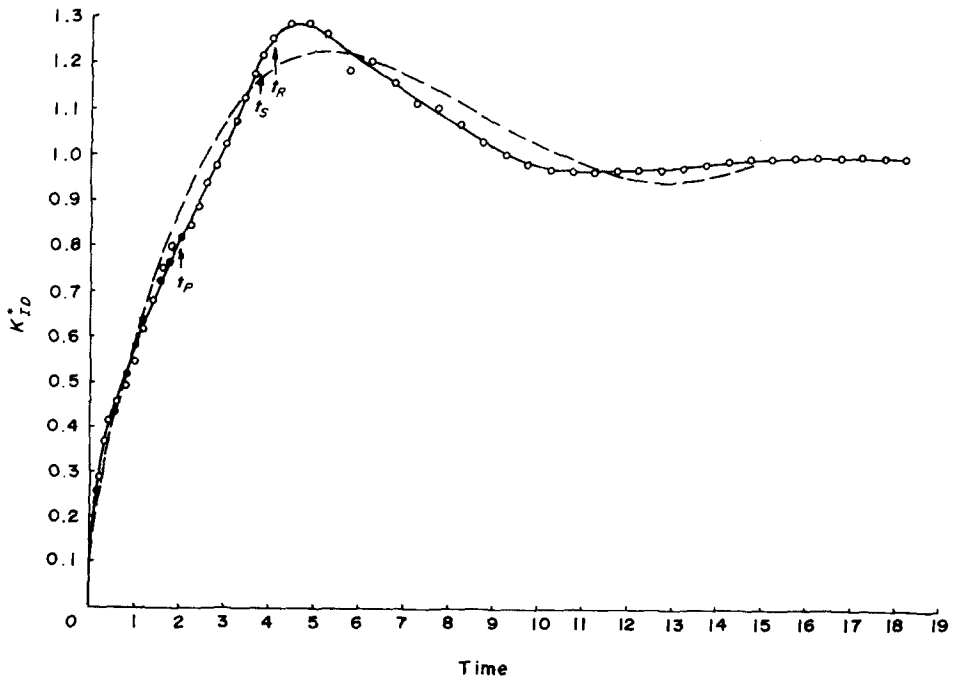


Fig. 7. The normalized dynamic stress intensity factor of a stationary crack $\kappa = 0.542$ ($\nu = 0.29$). ●; Baker[6]. ——; Sih *et al.*[14]. ——; This study. ○; $2N - 1 = 5$, $\Delta\tau = 0.2, 0.5$, $\Delta\eta^* = 0.2$.

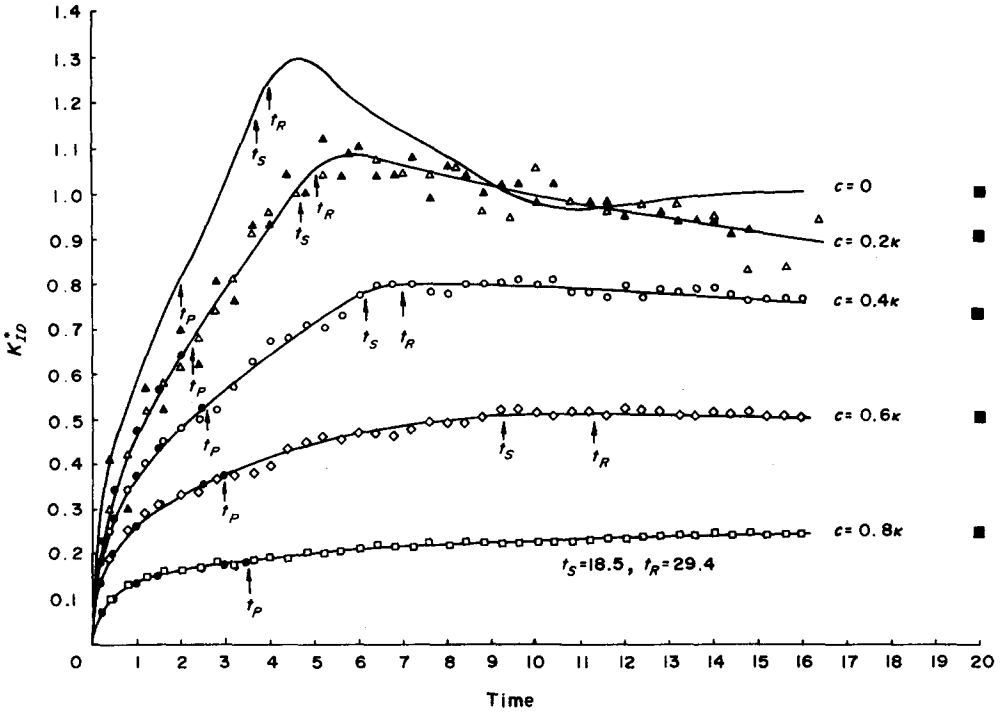


Fig. 8. The normalized dynamic stress intensity factor of a propagating crack with constant speed. $\kappa = 0.542$ ($\nu = 0.29$). ●; Baker[6]. ■; Broberg[7]. ——; This study. △; $2N-1=9$, $\Delta\tau = 0.4$–$0.8$, $\Delta\eta^* = 0.2$. ▲; $2N-1=5$, $\Delta\tau = 0.4$, $\Delta\eta^* = 0.2$. ○; $2N-1=9$; $\Delta\tau = 0.4$, $\Delta\eta^* = 0.2$. ◇; $2N-1=11$, $\Delta\tau = 0.4$, $\Delta\eta^* = 0.2$. □; $2N-1=9$, $\Delta\tau = 0.4$, $\Delta\eta^* = 0.2$.

where the values of $k(\kappa, c)$ for $\kappa = 0.542$ are obtained as follows:

| $c/\kappa$ | $k(\kappa, c)$ |
|---|---|
| 0.0 | 0.580 |
| 0.2 | 0.503 |
| 0.4 | 0.414 |
| 0.6 | 0.306 |
| 0.8 | 0.157 |

The results for the three example problems are discussed in the following:

(1) *Stationary crack*

The numerical results for $\kappa = 0.577$ are shown in Fig. 6 in comparison with Thau and Lu[13]. The time scale of their data is modified in Fig. 6 in such a way that the normalization is on the same basis as in this investigation. It is shown in [13] that if $\kappa$ is such that $t_R < t_{PP}$, $K^*_{ID}$ attains its maximum value ($\approx 1.3$) at $t = t_R$ and $dK^*_{ID}/dt$ approaches $+\infty$ as $t \to t_R-$ and it is finite as $t \to t_R+$. As one may observe, the two results agree quite well over the time period $0 < t < t_{PP}$. The sharp peak at $t = t_R$ is smoothed out in the present result due to the omission of the propagating logarithmic singularity in the computation process. The large time behavior of $K^*_{ID}$ is an agreement with the results in Sih *et al.*[14] as illustrated in Fig. 7.

(2) *Propagation with constant speed*

The $K^*_{ID}(t)$ curves for $\kappa = 0.542$ and a number of crack speeds are presented in Fig. 8. The results for $t < t_P$ agree well with Baker's results mentioned above. The large time solutions are compared with Broberg[7] in which a crack propagates symmetrically with constant speed from zero initial length under constant pressure on the crack face. $K^*_{ID}$ obtained from his equation for $\sigma_{yy}$ is given by

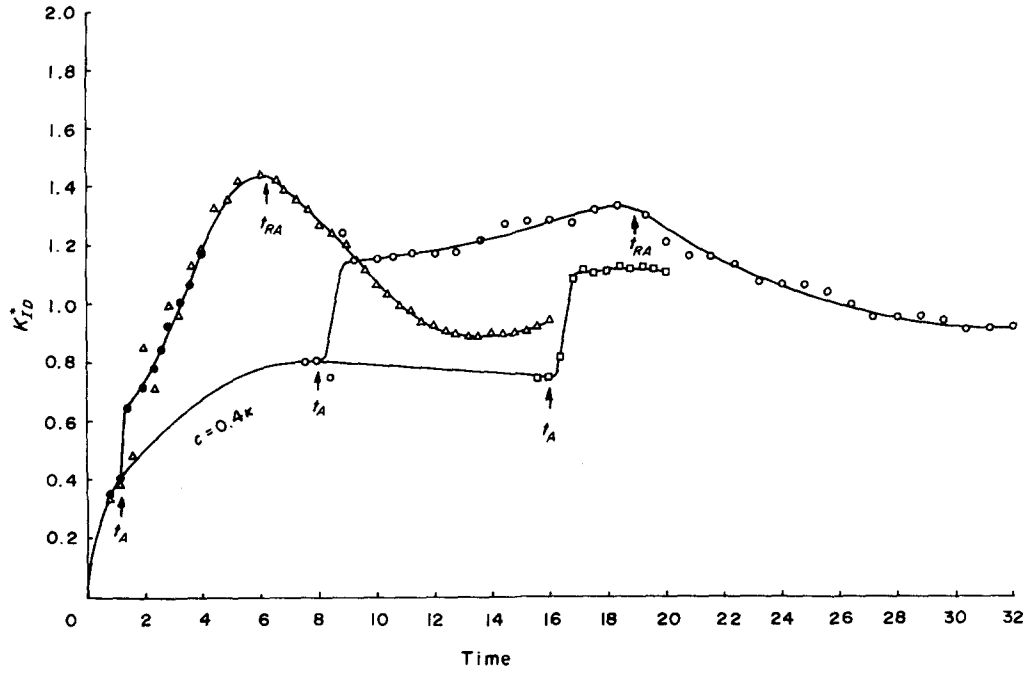


Fig. 9. The normalized dynamic stress intensity factor of a suddenly stopping crack after propagating with speed $c = 0.4\kappa$. $\kappa = 0.542$. ●; $2N-1=0$, $\Delta\tau = 0.1$, $\Delta\eta^* = 0.2$. △; $2N-1=9$, $\Delta\tau = 0.4$, $\Delta\eta^* = 0.2$; ○; $2N-1=9$, $\Delta\tau = 0.4$, $\Delta\eta^* = 0.2$. □; $2N-1=9$, $\Delta\tau = 0.4$, $\Delta\eta^* = 0.2$.

$$K^*_{ID} = \frac{1-c^2}{c^2 g(c)}\left[-\frac{(2\kappa^2-c^2)^2}{\sqrt{(1-c^2)}} + 4\kappa^3\sqrt{(\kappa^2-c^2)}\right] \tag{47}$$

where $g(c)$ is defined by eqn (25) in [7]. For $\kappa = 0.542$, the following numerical values are obtained:

| $c/\kappa$ | $K^*_{ID}$ |
|---|---|
| 0.0 | 1.0 |
| 0.2 | 0.905 |
| 0.4 | 0.723 |
| 0.6 | 0.505 |
| 0.8 | 0.243 |

It is observed in Fig. 8 that the values of $K^*_{ID}$ at large times approach Broberg's $K^*_{ID}$. This implies that the effects of the initial width of the crack become negligible as crack propagates. Another interesting phenomenon one can observe in this figure is that the maximum value of $K^*_{ID}$ is attained at $t \simeq t_R$, and that the overshoot of $K^*_{ID}$ beyond the large time $K^*_{ID}$ becomes insignificant as crack speed increases.

(3) *Suddenly stopping crack*

The behavior of $K^*_{ID}$ for a suddenly stopping crack is studied for $\kappa = 0.542$ and several values of $c$ and $t_A$. A typical result is presented in Fig. 9. In any case a jump discontinuity was found in $K^*_{ID}$ at $t = t_A$. The size of the jump and the values of $K^*_{ID}(t_A+)$ varied with the values of $c$ and $t_A$. The peak values of $K^*_{ID}$ were obtained approximately at $t = t_{RA}$. For $t > t_{RA}$, $K^*_{ID}$ decreases gradually and reaches 1 oscillating in a manner similar to the case of a stationary

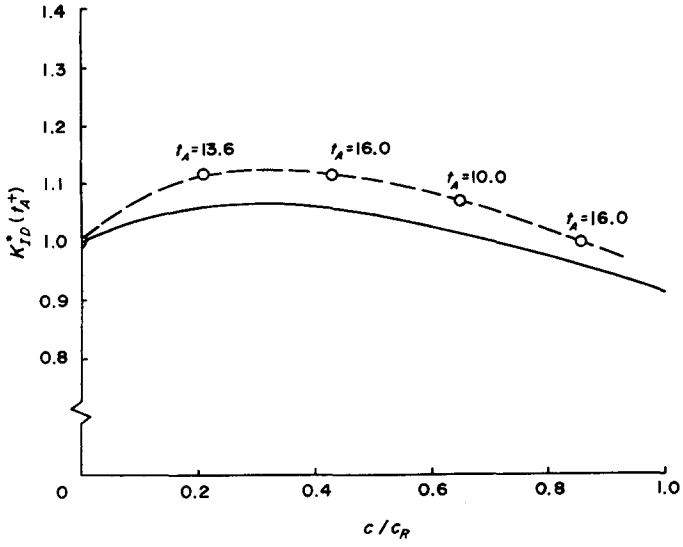


Fig. 10. The normalized dynamic stress intensity factor immediately after stopping of a Broberg crack vs crack speed/Rayleigh wave speed. ——; Freund[2], $\nu = 0.25$. ——; This study, $\nu = 0.29$.

crack. For sufficiently large values of $t_A$ at which Broberg's result is approximately reached $K^*_{ID}(t_A+)$ is compared with Freund[2] in Fig. 10. It is seen that the dependence of $K^*_{ID}(t_A+)$ upon $c/c_R$ is similar for the two cases.

*Acknowledgements*—The author wishes to express his gratitude to Dr. N. E. Ashbaugh, Prof. M. C. Stippes and Prof. D. S. Watanabe for valuable discussions and suggestions. This work was supported by the Nuclear Regulatory Commission through Battelle Memorial Institute.

## REFERENCES

1. J. D. Achenbach, Wave Propagation, Elastodynamic stress singularities, and fracture. *Proc. 14th IUTAM Congress* (Edited by W. T. Koiter) 71 (1976).
2. L. B. Freund, Dynamic Crack Propagation. *The Mechanics of Fracture* (Edited by F. Erdogan), *ASME-AMD*, Vol. 19, 105 (1976).
3. E. H. Yoffe, The moving Griffith crack. *Phil. Mag.* 42, 739 (1951).
4. J. W. Craggs, On the propagation of a crack in an elastic brittle materials. *J. Mech. Phys. Solids* 8, 66 (1960).
5. G. C. Sih and J. F. Loeber, Wave propagation in an elastic solid with a line of discontinuity or finite crack. *Quart. Appl. Math.* 27, 193 (1969).
6. B. R. Baker, Dynamic stresses created by a moving crack. *J. Appl. Mech.* 29, 449 (1962).
7. K. B. Broberg, The propagation of a brittle crack. *Arkiv. Fysik* 18, 159 (1960).
8. B. V. Kostrov, Unsteady propagation of longitudinal shear cracks. *Appl. Math. Mech. (PMM)* 30, 1042 (1966).
9. J. D. Eshelby, The elastic field of a crack extending non-uniformly under general anti-plane loading. *J. Mech. Phys. Solids* 17, 177 (1969).
10. L. B. Freund, Crack propagation in an elastic solid subjected to general loading—II. Non-uniform rate of extension. *J. Mech. Phys. Solids* 20, 1414 (1972).
11. J. D. Achenbach, Extension of a crack by a shear wave. *Z. Angew. Math. Phys.* 21, 887 (1970).
12. J. D. Achenbach and R. Nuismer, Fracture generated by a dilatational wave. *Int. J. Fracture Mech.* 7, 731 (1971).
13. S. A. Thau and T.-H. Lu, Transient stress intensity factors for a finite crack in an elastic solid caused by a dilatational wave. *Int. J. Solids Struct.* 7, 731 (1971).
14. G. C. Sih, G. T. Embley and R. S. Ravera, Impact response of a finite crack in plane extension. *Int. J. Solids Struct.* 8, 977 (1972).
15. J. D. Achenbach and Z. P. Bazant, Elastodynamic near-tip stress and displacement fields for rapidly propagating cracks in orthotropic materials. *J. Appl. Mech.* 42, 183 (1975).
16. L. B. Freund and R. J. Clifton, On the uniqueness of plane elastodynamic solutions for running cracks. *J. Elasticity* 4, 293 (1974).
17. N. I. Muskhelishvili, *Singular Integral Equations*. Noordhoff, Leyden (1953).
18. K. S. Kim, Elastodynamic analysis of a propagating finite crack. Ph.D. Thesis, University of Illinois (1977).